

# Torsional thrust stand for characterization of microthrusters

**K H Cheah<sup>1\*</sup> and K S Low<sup>2</sup>**

<sup>1</sup>School of Engineering, Taylor's University, Malaysia.

<sup>2</sup>Satellite Research Centre, School of EEE, Nanyang Technological University, Singapore.

\*keanhow.cheah@taylors.edu.my

**Abstract.** This paper describes the setup of a precise thrust stand based on torsional pendulum design for characterizing the performance of microthrusters. Calibration has been carried out by using an improved version of electrostatic calibrator, which produces a wide range of accurate and repeatable calibration force. After the calibration, the thrust stand can resolve constant force from 40 $\mu$ N to 3.4mN and impulse bit from 7 $\mu$ Ns to 340 $\mu$ Ns. The usefulness of the thrust stand has been demonstrated by measuring the performance of two different microthrusters: a pulsed plasma thruster that produces impulse bit of 23.15 $\mu$ Ns and a vaporizing liquid microthruster that produces steady state thrust of 633.5 $\mu$ N.

## 1. Introduction

In recent years, nanosatellites (<10 kg) have demonstrated their capability to carry out a wide range of missions at a rapid and cost effective way. The space community is very eager to send these satellites to perform more complex missions. Low thrust propulsion systems, which are often known as micro-propulsion systems, will benefit the complex missions in many ways. The propulsion systems can be used for routine activities such as attitude control, station keeping and drag compensation. They can also serve as the key enabling technology for advanced missions such as formation flying, proximity operations, rendezvous and docking with one another. In conjunction to this, thrust measuring tool that is able to resolve the forces in the order of micronewton is required for supporting the development of the various micropropulsion systems.

The most widely used instrument to directly measure the thrust from the micropropulsion systems is pendulum-type thrust stand. Three commonly used pendulum configurations are hanging pendulum, inverted pendulum and torsional pendulum. The hanging pendulum thrust stand [1, 2] is the easiest to set up. It is stable and least affected by the test conditions, e.g. change in flexural stiffness due to the thermal effect. However, it is also the least sensitive among the three configurations. To improve the sensitivity, a long pendulum arm is required. This poses difficulties to house the thrust stand in small facilities. In contrast, inverted pendulum thrust stand is highly sensitive and compact with the length of the pendulum arm as short as 20cm has been constructed [3]. Nevertheless, the compactness of the thrust stand makes it vulnerable to thermal expansion. In addition, the inverted design is very sensitive to the shift in centre of gravity of the thrust stand. Meanwhile, torsional pendulum thrust stand offers a good balance between the pros and cons of the other two configurations. It is relatively easy to set up and achieves high sensitivity with a reasonable pendulum arm. The arm rotational axis is parallel to the



gravity vector, making it less sensitive to the environmental noise. It is the most widely used pendulum thrust stand for performance characterization of various micropropulsion systems [4, 5-10].

This paper presents the setup of a torsional thrust stand based on improved version of electrostatic (ES) calibration system that has been previously developed in this research centre. By clustering a few heat sinks, generation of calibration force up to several tenths of mN is possible. This will improve the range of calibration force to four orders of magnitude. Accurate and repeatable calibration forces are produced by precisely controlling the voltages supplied to the calibrator. Practical applications of the thrust stand are demonstrated by using it to measure the performance of a pulsed plasma thruster and a vaporizing liquid microthruster.

## 2. Principle of thrust measurement

The motion of a typical torsional pendulum can be described by a second order differential equation as

$$J\ddot{\theta} + \lambda\dot{\theta} + k\theta = F_t r_t \quad (1)$$

where  $J$  is the moment of inertia about the rotational axis,  $\theta$  is the angular displacement of the pendulum,  $\lambda$  is the damping coefficient,  $k$  is the torsional elastic constant and  $F_t$  is the externally applied force at a distance of  $r_t$  from the rotational axis.

When an impulsive force with magnitude of  $F_i$  is applied on the pendulum for a duration of  $t_i$ , the external force can be expressed as:

$$F_t = \begin{cases} 0 & t < 0 \\ F_i & 0 \leq t \leq t_i \\ 0 & t > t_i \end{cases} \quad (2)$$

The general solution for the motion of pendulum after applying impulsive force,  $t > t_i$ , is given as:

$$\theta(t) = \frac{r_t F_i t_i}{J \omega_o} e^{-\frac{\lambda t}{2J}} \sin(\omega_o t) \quad (3)$$

where  $\omega_o$  is the natural frequency of the pendulum.

From the sinusoidal function in (3), the maximum angular displacement is given by:

$$\theta_{\max} = \frac{r_t F_i t_i}{J \omega_o} \quad (4)$$

Comparing to angular displacement, the linear displacement of the pendulum,  $\Delta x$ , can be measured easily using an optical sensor. From small angle approximation, displacements can be correlated by:

$$\Delta x = r_{LDS} \theta \quad (5)$$

where  $r_{LDS}$  is the distance between the linear displacement sensor and the rotational axis

Combining (4) and (5), the impulse bit can be expressed by:

$$I_{bit} = F_i t_i = \frac{J \omega_o}{r_t r_{LDS}} \Delta x_{\max} \quad (6)$$

When constant force,  $F_c$ , is applied on the pendulum, the pendulum motion is simply described as:

$$F_c r_t = k \Delta \theta \quad (7)$$

where  $\Delta \theta$  is the steady state angular displacement of the pendulum caused by the force. Rearranging and considering (5), the constant force is expressed as:

$$F_c = \frac{k}{r_t r_{LDS}} \Delta x \quad (8)$$

where  $\Delta x$  is the steady state deflection of the pendulum caused by the force.

From (6) and (8), it is evident that a thrust stand based on torsional pendulum principle can be set up to evaluate the impulse bit and constant thrust from different thrusters with the prior knowledge of  $J$ ,  $\omega_o$  and  $k$ . These parameters are sensitive to the changes in configuration of the thrust stand. For example, distribution of weight in the thrust stand affects  $J$  and  $\omega_o$  while the effective  $k$  is influenced by electrical wiring.

Instead of evaluating each of these parameters separately, a calibration process is carried out to establish the relationship between the thrust stand response and the applied impulse bit or constant force. Using the calibration approach, all of these parameters are accounted for under the parameter of sensitivity,  $S_{cal}$ . It simplifies the measurement of impulse bit from a thruster as:

$$I_{bit} = \frac{(L_{cal}/L_t)}{S_{cal,I_{bit}}} \Delta x_{range} \quad (9)$$

where  $L_{cal}$  and  $L_t$  are the distance between rotational axis to calibrator and thruster, respectively,  $S_{cal,I_{bit}}$  is the sensitivity of thrust stand to impulse bit,  $\Delta x_{range}$  is the maximum peak-to-peak displacement of the thrust stand.

Similarly, the constant thrust from a thruster can be evaluated by:

$$F_c = \frac{(L_{cal}/L_t)}{S_{cal,F_c}} \Delta x_t \quad (10)$$

where  $S_{cal,F_c}$  is the sensitivity of thrust stand to constant force and  $\Delta x_t$  is the steady state deflection of the thrust stand.

In a particular test set up, the  $L_{cal}$  and  $L_t$  are always fixed. To find out the sensitivity, a number of known calibration impulse bits or constant forces are applied to the thrust stand. The corresponding thrust stand responses ( $\Delta x_{range}$  or  $\Delta x_t$ ) are recorded and plotted as a calibration curve. The linear relationship between the calibration force and the thrust stand response allows the sensitivity of the thrust stand to be computed from the gradient of the curve.

### 3. Setup of torsional thrust stand

A horizontal pendulum type thrust stand in symmetrical configuration is designed and set up. The balance consists of a rotating platform, a central pillar which houses the pivot and a heavy base plate for mounting of other accessories. The rotating platform is made of aluminium alloy beam of 60cm long. The thruster is mounted on one end while a counterbalance mass and an electrostatic calibrator are placed on the other end. The platform is attached to a pivot through the central pillar. This limits the motion of the platform to one degree of freedom only as shown schematically in Figure 1.

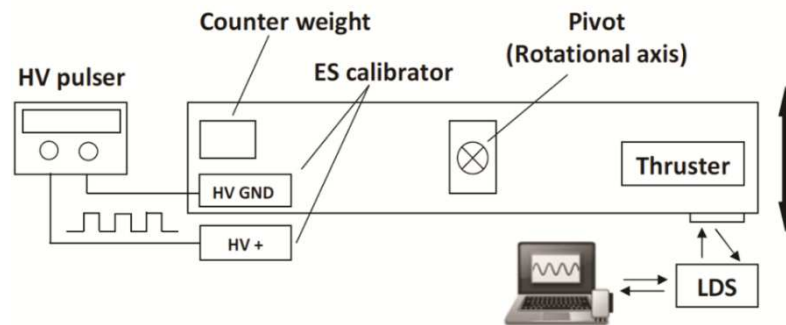


**Figure 1.** Schematic of the setup of torsional thrust stand

A stainless steel double-ended flexural pivot (6012-400, Riverhawk) was chosen. It demonstrates significant advantages over conventional bearings. The pivot is frictionless, requires no lubricant and almost maintenance-free. A strong permanent magnet with adjustable height was placed on one end of the platform to induce passive magnetic damping force of different magnitudes on the rotating platform.

An optical sensor (ILD 2300-2, MicroEpsilon) based on the principle of laser triangulation was used for linear displacement measurement. The non-intrusive and optical nature of the sensor is advantageous as it is not susceptible to electromagnetic interference [11]. This sensor has measuring range of 2mm and resolution as low as 30nm at measuring rate of 20kHz.

A non-contact calibration technique based on the principle was implemented. An improved version of the system based on 2D array of electrostatic fins was developed in our centre. The system is very compact and weighs only 23g. A detailed description of the improved system and its capability to produce a wide range of accurate and repeatable calibration force has been reported in our previous work [12]. In general, the ES calibrator system consists of a set of two 2D ES fin assemblies which engages for a particular distance as illustrated in Figure 2. By controlling the applied voltage precisely, it has been experimentally demonstrated that the calibration forces produced at 2mm difference of engagement distance are within 2% of deviation.

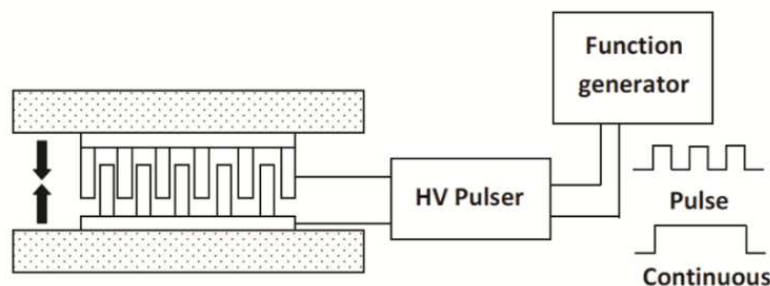


**Figure 2.** Schematic of electrostatic calibrator

A high voltage (HV) pulser (PVM-4210, DEI) supplies the required potential difference between the ES fin assemblies. The maximum voltage was limited to 900V to avoid arcing between the fin assemblies. Measuring with precision weighing balance, the ES calibrator system produces calibration force in the range of  $40\mu\text{N}$  to  $3.4\text{mN}$  consistently with deviation error less than 2%. Calibration impulse bit in the range of  $7\mu\text{Ns}$  to  $340\mu\text{Ns}$  was produced with error within 5%. For setting up the calibrator system on the torsional balance, one fin assembly was mounted on one end of the rotating platform while another fin assembly was fixed externally.

A vacuum facility has been set up not only to produce a vacuum environment required for the operation of electric thrusters but also to simulate the space environment for future testing of other thruster systems. The vacuum chamber is 70cm in diameter, 100cm in length and made of stainless steel. Vacuum solution for the chamber consists of a turbo pump (HiPace400, Pfeiffer Vacuum) and backed by a rotary vane pump (DUO65M, Pfeiffer Vacuum). An ultimate vacuum level in the order of  $10^{-6}$  mbar is achievable. Throughout the testing, the chamber pressure is maintained at the level of  $10^{-5}$  mbar.

#### 4. Characterization of microthrusters

The versatility of the thrust stand to measure both impulse bit and constant thrust was demonstrated. It was used to characterize the performance of two different micropropulsion systems developed in our centre.

##### 4.1. Pulsed plasma thruster

Pulsed plasma thruster (PPT) is an electric propulsion system that operates in pulse mode. When the PPT operates, it discharges the energy stored in the capacitor bank to ablate and ionize the solid teflon propellant to become plasma. Simultaneously, the flowing of high intensity electrical current during the discharge induces a strong magnetic field which accelerates the plasma to a velocity as high as a few km/s. From Newton's laws of motion, this produces an impulse bit in the opposite direction to the accelerated plasma.

Before the impulse bit measurement, the calibration process was carried out. The voltage input to the ES calibrator was fixed at 500V. The HV pulse width was varied from  $16\mu\text{s}$  to  $50\mu\text{s}$  for producing different impulse bits on the thrust balance. The resulting calibration curve as shown in Figure 3(a) was plotted after recording the thrust stand responses. Subsequently, a single PPT shot of unknown impulse bit was triggered. A typical thrust balance response to the PPT shot is shown in Figure 3(b). 10 measurements were taken and the average maximum displacement is  $15.07\pm 0.51\mu\text{m}$ . From the average maximum displacement and the sensitivity of the balance derived from the calibration curve, the impulse bit was evaluated as  $23.15\pm 0.79\mu\text{Ns}$ .

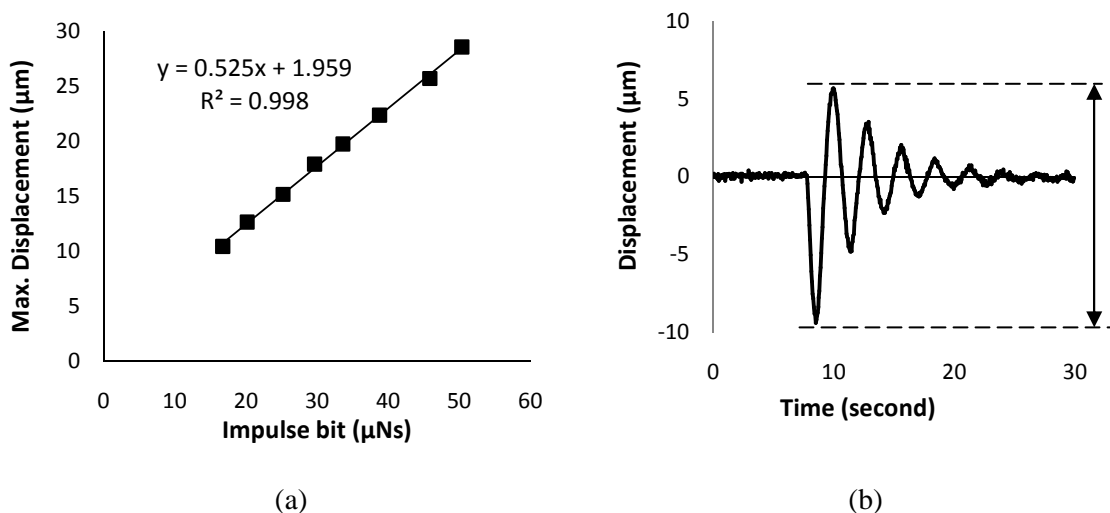


**Figure 3.** (a) Calibration curve for PPT impulse bit measurement, (b) thrust stand response to a single PPT shot. The arrow shows the maximum displacement

##### 4.2. Vaporizing liquid microthruster

Vaporizing liquid microthruster (VLM) is a liquid propulsion system. Figure 4(a) shows a MEMS-scale VLM made of ceramic material [13]. Liquid propellant is injected into the microthruster using a

syringe pump at a controlled flow rate. When sufficient electrical power is applied, the liquid propellant was vaporized. The hot vapor is ejected from the microthruster through the micronozzle as shown in Figure 4(b). A continuous force is produced when the liquid propellant is continuously fed into the microthruster while sufficient electrical energy is supplied.

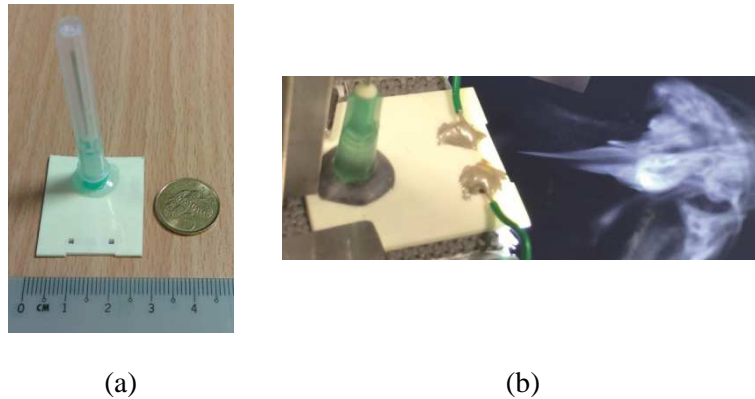


**Figure 4.** (a) Ceramic MEMS-scale VLM developed in SaRC, NTU. (b) Operation of VLM using water as propellant. Ejected water vapor is made visible using an appropriate lighting.

Similarly, calibration process was carried out prior to the thrust measurement. Different known calibration forces were applied on the thrust balance. The corresponding steady state deflection were recorded and plotted into the calibration curve in Figure 5(a). Then, the liquid propellant was fed in and the power supply was switched on. After approximately 10 seconds of operation, a steady state operation is achieved. The thrust balance was deflected for  $128.56\mu\text{m}$  as shown in Figure 5(b). Considering the sensitivity from the calibration curve and using (9), maximum thrust of  $633.5\mu\text{N}$  was produced at  $1\mu\text{l/s}$  of flow rate.

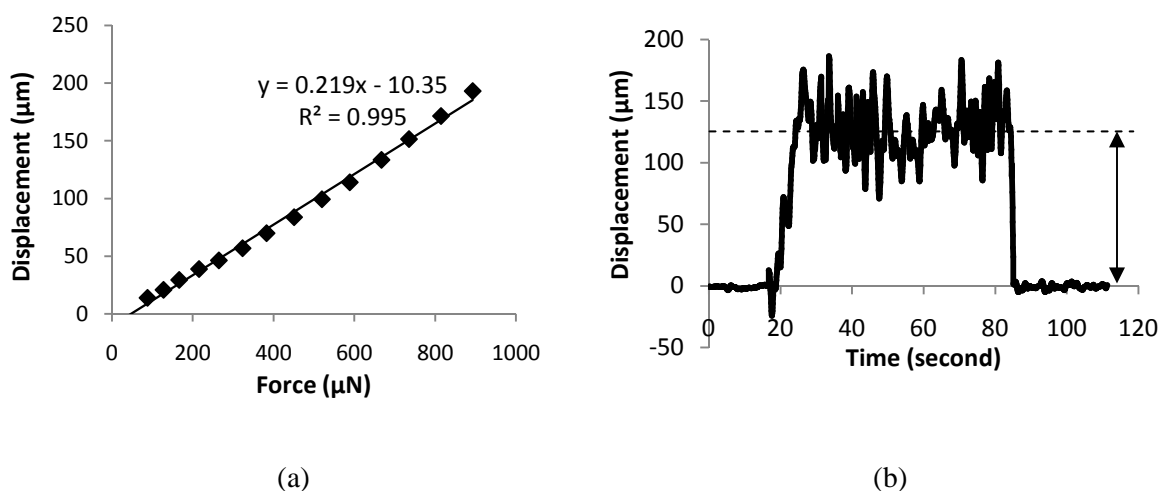


**Figure 5.** (a) Calibration curve for VLM constant thrust measurement, (b) Thrust stand response to operation of VLM

## 5. Conclusion

Development of a precise torsional pendulum thrust stand that can resolve forces in the order of micronewton has been presented. The thrust stand was set up as diagnostic tool for characterizing the performance of micropropulsion systems developed in SaRC, NTU. The thrust stand has been used to

measure the performance of two microthrusters developed in our centre. The pulsed plasma thruster produces impulse bit of  $23.15\mu\text{Ns}$  at 1Hz. The vaporizing liquid microthruster produces a steady state thrust of  $633.5\mu\text{N}$  by consuming water propellant at  $1\mu\text{l/s}$ .

### References

- [1] Polzin K A, Markusic T E, Stanojev B J, Dehoyos A, and Spaun B 2006 *Rev. Sci. Instrum* **77** 105108
- [2] Rocca S 2011 *Aerosp. Sci. Technol* **15** 148
- [3] Haag T W 1991 *Rev. Sci. Instrum* **62** 1186
- [4] Gamero-Castano M 2003 *Rev. Sci. Instrum* **74** 4509
- [5] Ciaralli S, Coletti M and Gabriel S B *Meas. Sci. Technol* **24** 115003
- [6] Koizumi H, Komurasaki K and Arakawa Y 2004 *Rev. Sci. Instrum* **75** 3185
- [7] Lun J and Law C 2014 *Meas. Sci. Technol* **25** 095009
- [8] Zhou W J, Hong Y J and Chang H 2013 *Rev. Sci. Instrum* **84** 125115
- [9] Zhang D, Wu J, Zhang R, Zhang H and He Z 2013 *Rev. Sci. Instrum* **84** 125113
- [10] Yang Y X, Tu L C, Yang S Q and Luo J 2012 *Rev. Sci. Instrum* **83** 015105
- [11] Cubbin E A, Ziemer J K, Choueiri E Y and Jahn R G 1997 *Rev. Sci. Instrum* **68** 2339
- [12] Cheah K H, Low K S, Tran Q V and Lau Z 2015 *IEEE T. Instrum. Meas* **64** 3467
- [13] Cheah K H and Low K S, Tran Q V and Lau Z 2015 *J. Micromech. Microeng* **25** 015013